
Article:
Sunar, O. orcid.org/0000-0002-8830-7570, Fletcher, D. orcid.org/0000-0002-1562-4655 and Beagles, A. (2021) Laboratory assessment of arc damage in railway overhead contact lines with a case study on copper-silver and low oxygen content copper. IEEE Transactions on Power Delivery, 36 (5). pp. 3074-3081. ISSN 0885-8977

https://doi.org/10.1109/tpwrd.2020.3032798

Laboratory assessment of arc damage in railway overhead contact lines with a case study on copper-silver and low oxygen content copper

Özgün Sunar, David Fletcher, Adam Beagles

***Abstract*— New laboratory-based test equipment is described for controlled arc exposure of short lengths of railway electrification contact wire (100 mm) enabling a rapid and low-cost experimental investigation of electric arc damage due to loss of contact between the pantograph and overhead line. The extreme local heating typical of arc sites is found to locally reduce wire hardness, seeding sites for wear and fatigue crack initiation. Contact loss may be produced by poor dynamic behaviour at the pantograph to overhead line interface, often caused by changes in system stiffness or local misalignment of the overhead line. In this study, arcs were generated with computer control of pull away and approach to the wire to carbon strip contact, with peak currents in the range 100 to 200A for direct current and ± 200A for alternating current. Metallurgical and mechanical damage identified is correlated against energy input quantified through voltage and current measurements. Interior void formation within the contact wire and modification of grain size are revealed with optical microscopy, metallography, surface mapping and microhardness tests. Initial tests using the new equipment with two materials show the potential for investigating mitigation of arc damage by changing contact wire composition.**

***Index Terms*—arcing, overhead line, contact wire**

I. Introduction

Railway overhead line electrification (OLE) systems include contact wires that transmit energy to trains through contact with the pantograph. The pantograph exerts an uplift force which is reacted by the contact wire, and the system is designed to maintain continuous contact. Figure 1 shows the pantograph contact wire system in OLE mainlines. Both mechanical wear and electrical transmission at this interface impact component life. In particular, momentary loss of physical contact between the pantograph and the overhead contact wire produces arcing and consequent extreme local heating in the contact wire. This may be due to poor pantograph dynamics or wire misalignment and can also occur while crossing neutral sections and section insulators that are provided to isolate different electrical sections of overhead lines. Besides pantograph arcing, the contact wires that may pass close to structures, especially if OLE is retrofitted to existing non-electrified lines. There can be particularly limited electrical clearances when the system passes bridges, overpasses or tunnels which were not originally designed to accommodate the wires. This can result in "flashover arcing" between live wires and supporting or external structures [1]. Plates or strips are used to prevent bridges or overpasses from being damaged, but flashover can also damage OLE contact wires at the locations where the electrical discharge occurs. Although arcing almost always lasts less than a second, the temperature of the contact wire may be elevated to reach its melting temperature.

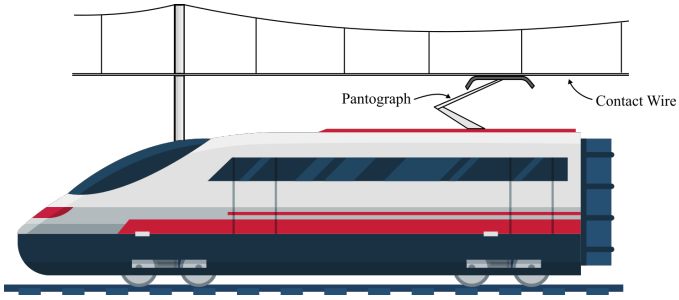

Figure 1 Schematic of the overhead line equipment

Studies in the past have provided important information on pantograph-contact wire arcing [2]–[5]. Some of these studies reflected a concern that there would be increased arcing associated with increasing train speed. This problem was highlighted during the wear investigation of pantograph carbon strips by Kubo et al. [6] in which it was stated that the thermal effects of discharge could result in melting and evaporation of copper. Sliding contact with poor dynamics resulting in arcing is described as an "electrical welding" effect by Gonzalez et al. [7] and He et al. [8].

Bucca et al. [9] discussed the three main contributions to the wear rate of pantograph and contact wire: mechanical, electrical, (Joule effect) and electrical arcs due to power dissipation generated by the electrical arcs that occur when the contact dynamics cause a loss of contact. Several studies have used a rotating disc to examine the air gap between pantograph and contact wire. The varying gap between electrodes due to mechanical vibration was identified as the main reason for pantograph arcing by Wang et al. [10]. They also highlighted that pantograph arcing could cause ablation of the contact wires and shorten their life. This view was supported by He et al. [11] who wrote that it is inevitable that contact wires soften due to arcing regardless of the polarity of contact wire-pantograph systems. According to a study by Wang et al. [12], the main causes of arcing were poor mechanical contact, shape irregularities of the contact wire and the influence of high-speed airflow.

Wei et al. [13] termed the types of arcs as drawn or approaching arcs these occur when mechanical contact breaks and reforms, respectively. It was found that the intensity of the drawn arc is much stronger than that of the approaching arc. Also, Yang et al. [14], Kubo et al. [15] and Jia et al. [16] showed

that the accumulated arc discharge energy can be calculated as follows [17]:

$$E_a = \int UIdt \quad (1)$$

where E_a is the accumulated arc energy (Joules), U is the arc voltage drop between the contact strip and contact wire (Volts), I is the electric current flowing through the friction pair (Amperes), and t is time (seconds).

The primary purpose of most of the studies identified was quantifying and understanding damage to the pantograph current collection surface. However, there is a relatively small amount of literature that is concerned with arc damage effects on the contact wire. Yang et al. [3] and Ding et al. [18] found that there can be an extensive temperature rise due to arcing, exceeding that generated by friction. Zhu et al. [19] examined the temperature distribution generated by an arc discharge between the pantograph and contact wire surface with currents between 100-300 A. The results showed that during the current flow copper on the surface melts and turns into vapour due to the high temperature.

In studies on copper-based materials outside contact wire but relevant to the experimental results in Section III, void formations and defects have been found in the heat affected area during studies into the weldability of copper materials, this phenomenon first being described as 'Hydrogen Sickness' by Butomo et al. in 1968 [20]. It was found that when copper alloys containing up to 0.01% oxygen in the form of Cu_2O were subjected to heat treatment in an atmosphere containing hydrogen, there was potential for a reaction between Cu_2O and H_2 producing Cu and H_2O. Nagata [21] identified this issue as 'hydrogen embrittlement' finding that it resulted in oxide depletion or holes at the sites of cuprous oxide particles, particularly above 375 °C (the critical temperature of the water, easily exceeded during arcing) where water can only exist as steam. The same phenomenon is described as 'hydrogen attack' in a study from Louthan [22] describing the formation of steam pockets or bubbles within the material. Similarly, Lutava [23] identified that water vapour could develop a high enough pressure to form pores in copper.

The studies in the literature thus far provide evidence that arcing plays an important role in the life and safety of OLE components. Studying this on an installed system during the passage of a train would provide realistic experimental conditions but with many uncontrolled variables such as the environmental humidity or wind speed. Testing would also be slow since any location would only see one potential arc with each pantograph passage. Laboratory-based systems using a rotary contact wire track [24]–[27] have been designed primarily to investigate the impact of wear (including wear due to arcing) of pantograph collector strips and as with testing on a real system would face difficulties in generating arcs on a specific part of their copper contact wire. A need was therefore identified for a new approach focusing on the contact wire, aiming to subject it to an arc in a specific location, ideally without consuming large lengths of wire for each test. In this paper, a new test machine to support an investigation of arcing phenomena is described, focusing on metallurgical and mechanical changes to the running surface and heat-affected zone of overhead contact wires. The study of arcing is undertaken without mechanical wear, although arc exposed samples can be subjected to secondary testing for wear and fatigue implications of arc exposure. The test machine is designed to use only small quantities of contact wire and collector strip in each test, making it easier to explore a wide range of materials and conditions at low cost, for example, to investigate the potential for mitigation of arc damage by changing contact wire composition.

II. Materials and Methods

A. Experimental Configuration

A new overhead line arc testing machine, Sheffield Overhead Line Arc Machine (SOLARC) that can accommodate any railway contact wire cross-section was designed (Figure *2*). The machine takes contact wire in the standard diameter range 10-15 mm as supplied for installation by the manufacturer. It allows the air gap, current, current type and arc durations to be controlled.

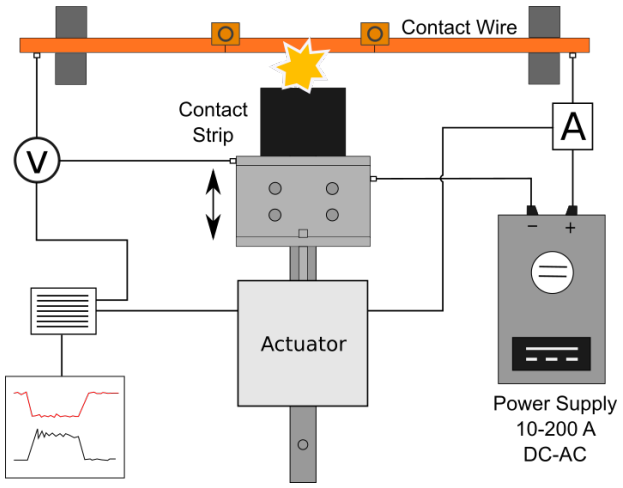

Figure 2 Schematic of SOLARC overhead line arc exposure test machine

A section of current collection strip housed in a linear guide is used for the pantograph side of the contact, with contact and break motions driven by a linear solenoid actuator. This is designed to reproduce the separation of the pantograph and contact wire but is not intended to replicate the full dynamics of the contact. Carefully alignment of the wire parallel to the collector strip surface was undertaken in each test to create a configuration representative of service. An adjustable power supply running from laboratory 230V AC mains provides either direct or alternating current with the maximum voltage of 80 V DC and ± 80 V AC and a peak current configurable from 10-200 A for DC and ± 200 A for AC. This voltage is representative of those measured across arcs in overhead line electrification installations [13] but clearly is not the full system voltage which is typically 25kV for AC systems or 750-1500V for DC systems. The configuration is able to represent full contact (close to zero voltage across the carbon to contact wire,

with a large current flowing), arcing and drawn arcs (~80V between the components with a large current flowing). It is not intended to reproduce an approaching arc since the potential difference is insufficient to start an arc until the components are virtually in contact. The experimental work, therefore, focuses predominantly on drawn arcs, such as would occur where a pantograph loses contact with a misaligned contact wire.

A current probe and voltmeter were attached to the equipment to monitor the current and voltage variation at the contact during the experiments. Duration, interval and number of arcs were controlled by a programmable microcontroller. This controller sent signals to a linear solenoid that attached to the carbon material cut from the pantograph carbon strip. Real-time position monitoring of the carbon strip that was attached to the actuator was recorded using a high-speed camera system. Afterwards, the experimental testing samples were investigated metallurgically and mechanically to quantify the effects of the arc and consequent damage to the contact wire.

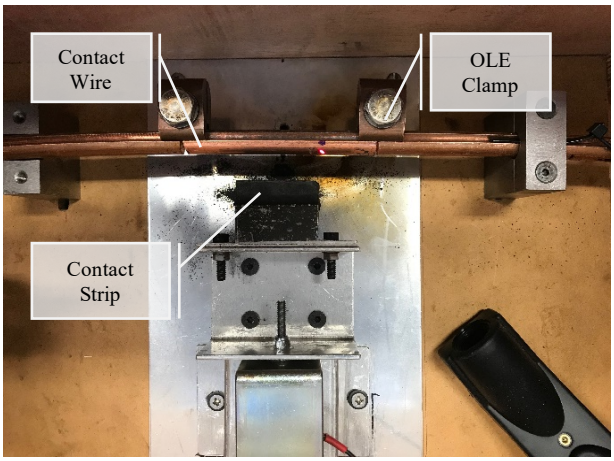

Figure 3 Photograph of SOLARC working area with contact wire connection and clamps

The machine can accommodate specimens up to 400 mm long, but a standard test specimen of 100mm length was used throughout the testing described below, this being sufficient to expose the surface to an arc without any influence from the supports or clamps. This small specimen length avoids large amounts of material from being wasted (Figure *3*). The typical electrical resistance of Cu-Ag overhead line contact wire with a nominal content of 0.1% silver and 0.04 % oxygen by weight is given by standard EN 50149 [28] as 0.122 Ω/km, and its manufactured hardness as 120HV. In the experiments, newly manufactured copper-silver contact wires were used (unworn and free of discolouration or significant surface oxide layers), along with very low oxygen content copper (typically referred to as “oxygen-free” copper, OFC) containing 0.0005 % oxygen [29].

B. Arc Experiments

Copper-silver contact wires from production deliveries of wire for railway installation were used to gain an understanding of the damage mechanisms during arc exposure for current materials in railway overhead contact wires. The potential to prevent or reduce this damage was explored by testing the OFC material. It was not possible to obtain a contact wire form of oxygen-free copper (OFC) since it had not yet been widely commercialised. Therefore, the OFC was a stock material rather than a contact wire, so its initial grain structure did not have the highly aligned configuration characteristic of a drawn material. This difference is referred to below when interpreting the results.

The specimens were subjected to arcing in the SOLARC machine with a pantograph collector to wire electrical contact time of 150 ms, achieving this to ± 20 ms. This variation was due to the arc being sustained for slightly different durations even when the actuator was operated in the same way. Tests were conducted as summarised in Table 1. All tests began with the contact wire and carbon strip out of contact, as they moved into contact, there was the possibility of an approaching arc. A period of contact was followed by separation and formation of a drawn arc. All tests took place under indoor laboratory conditions. Sliding interaction between pantograph carbon and contact wire was not represented in the tests. Tests T1, T3 and T6 exposed the contact wire to a single arc with AC or DC. Tests T2, T4 and T7 considered repetitive arc exposure, such as might occur at neutral sections or section insulators where arcs are more likely to happen. For these multiple arc tests, the time between the arcs was chosen to prevent unrealistic heating of the contact wire surface and to represent a typical high-capacity railway line. Test T5 represented arcing from both front and rear pantographs of a double pantograph train. In this test, the interval between arcs was set based on a 125-metre pantograph separation for a train travelling at 125 km/h.

Table 1 Parameters used in the experiments

Test ID	Current [A]	Number of Arcs	Time Between Arcs	Test Repeat	Power Supply
T1	100	1	-	4	DC
T2	100	10	2 min	4	DC
T3	200	1	-	4	DC
T4	200	10	2 min	8	DC
T5	200	2	3.6 sec	4	DC
T6	200	1	-	6	AC
T7	200	10	2 min	6	AC
T8	200	10	2 min	4	DC
T9	Thermal processing annealed for 2 hours at 450° C				

Test T8 investigated the effects of contact wire oxygen content on void formation in the material. This test was conducted with OFC material and a repetitive arc exposure with 200 A DC. To understand why the grain sizes changed and how heating modifies as-manufactured grains, in test T9 a none arc exposed contact wire was annealed. For pure copper, the recrystallisation temperature is just over 250°C, but the addition of silver raises this to 450°C, and this temperature was held for 2 hours. Grain sizes were investigated using an optical microscope with an average grain size determined according to standard ASTM E112-13 [30].

C. Metallography

The metallurgical examination was used to gain a detailed

understanding of the effect of arc(s) on the contact wire, both at the surface and internally. Following experimental testing contact, wire samples were prepared for examination by cutting parallel to the longitudinal axis to reveal the internal cross-section perpendicular to the surface and below the arc location. This allowed examination (microscopy, micro or nano-indentation and hardness testing) from the contact surface to the interior. Figure 4 shows the sectioning direction of the contact wire samples for metallography.

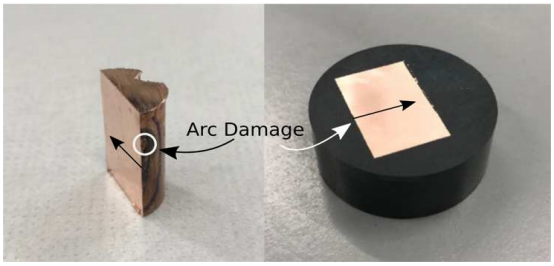

Figure 4 Longitudinal-vertical section through the contact wire. Straight arrows indicate the path for hardness profile measurements through the interior of the sample

To reveal the heat-affected zones and grain boundaries final polishing was completed with a 0.06 µm silica suspension and specimens were etched with a solution of 5 g FeCl3 in 96 ml industrial methylated spirits (IMS) with 2 ml HCl. Grain properties showed differences between the contact surface and interior of the material, so care was taken not to over-etch the heat-affected region; this was found to react faster to the etchant than material towards the centre of the wire.

III. Results

A. Voltage-Current Measurements

Fig. 5 shows the current and voltage variations during tests T3 and T4, and the corresponding position of the contact strip over time. The graphs show three stages, namely; approaching arc (I), full contact (II) and drawn arc (III). Fig. 4(a) shows the voltage-current measurements for test T3, which ran at 200 A DC. In stage I, the collector strip moved towards the contact wire, the voltage between them dropped sharply to zero as contact was made and the current rose to just over 200 A. Once mechanical contact was established current remained at just over 200A and voltage remained very close to zero in stage II during which good contact was maintained. In stage III a drawn arc developed when the mechanical contact broke. The uni-directional current was maintained throughout from the DC supply but significant current fluctuation was measured between zero and 200A, with average current 132.6 A and voltage 40 V in the representative test shown in Figure *5* (a). The drawn arc lasted for an average of 300 ms across the tests. After stage III the contact wire to collector strip pair was fully separated and the voltage across the contact rose to a maximum of 70 V with no current flow.

For the AC system, the motion command of the collector strip was unchanged, but arc durations were greatly reduced. Figure *5* (b) shows a typical voltage and current graph in test T4. Open circuit peak voltage (V_{peak}) was around 70 V and RMS voltage (V_{RMS}) was 49 V. In stage I of the AC test an approaching arc was observed in the period of 30 ms. Peak current (I_{peak}) was just below 200 A. In stage II mechanical contact between the collector strip and contact wire was established. The voltage between them remained zero throughout the period. Peak current (I_{peak}) fell slightly to 185 A. In stage III as the collector strip moved away from contact wire a drawn arc was produced, lasting for 20ms. During this period, the voltage increased slightly from zero to 17 V.

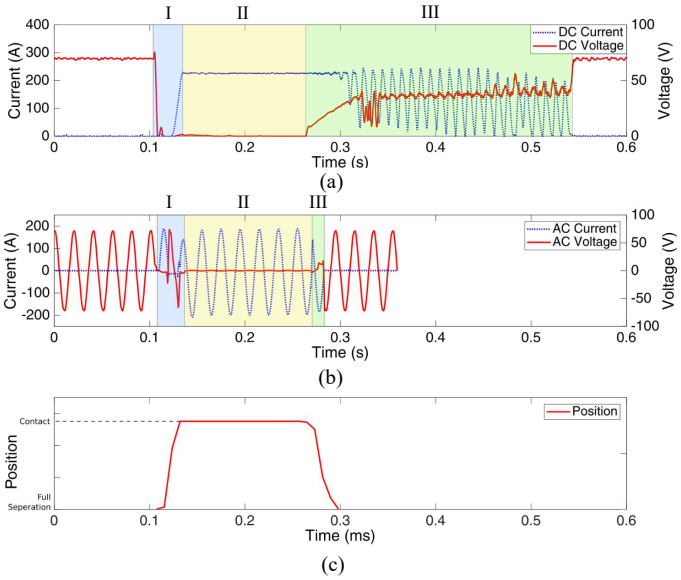

Figure 5 Voltage and current characteristics of arcing and the corresponding position of on contact strip a) 200 A DC b) 200 A AC c) Position of collector strip

The movement of the collector strip was identical for both AC and DC tests; however, the duration of the arcs varied. In particular, the drawn arcs in the DC tests lasted longer than the ones in AC tests. The accumulated energies expended in the arcs for both AC and DC cases were calculated from the current and voltage data and are given in Table 2. As the thermal conductivity of the pantograph carbon strip material is considerably smaller than that of the contact wire (398 W/mK contact wire, 6 W/mK pantograph carbon material) [22], energy dissipated in the pantograph carbon strip material was neglected. As would be expected, the accumulated energy was nearly zero in the regions of good contact and full separation due to zero voltage or current values. The results provided a means to correlate damage observed by microstructural examination (Section III.B) with the Joule heating during in arcing.

B. Arc Damage, Microstructure and Void Formation

Fig 6a shows a typical drawn arc (this example being from DC test T3) and Fig 6b shows marks generated on the contact wire surface by arcing. Strong arc discharge was observed with currents of both 100 and 200 A. After the carbon strip moved

(a)

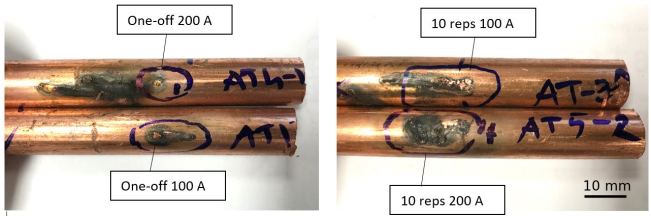

(b)

Figure 6 a) DC arc appearance during the experiments b) Burn marks on the surface of contact wire samples

away from the contact wire, the arc lasted approximately 300 ms before self-extinguishing. The size of the burn mark from a single arc was measured to cover an average of 2.2 mm along the wire length. It was seen that multiple arcs affected a wider area than single arcs, with the burn area extended longitudinally in the test numbers of T2 and T4.

Since the first arc modifies the wire surface (and will also modify the contact strip surface), it is to be expected that subsequent arcs may move to slightly different areas of the nominal contact between the surfaces. The surface modification inherent in the process means subsequent arcs between the same samples frequently affect a slightly different location across the nominal contact area than the first arc. Tilting the carbon to present a more definite single point of contact would eliminate this issue, but at the expense of reducing how realistic the apparatus was in replicating the pantograph-wire contact. This tilted carbon approach was therefore not adopted.

Figure *7* shows the sequence of microstructural images of contact wire samples. The grains in the initial microstructure of arc-free contact wire samples (Figure *7*a) were elongated parallel to the longitudinal axis of the contact wire, i.e. they had a high aspect ratio. The severity of visible damage from the surface to the interior of the contact wire varied depending on the current and number of arcs as shown by (Figure *7* b,c,d,e). There was a significant positive correlation between the arc current and the depth of transition between the visible HAZ and parent material. Hardness measurements (Section C.III) indicate that modification of the material reaches deeper than this visible transition. After being subject to an arc it was found that the grain structure was modified, and voids were seen both close to the surface and in the interior of the material. The grains in the visibly heat-affected zone (HAZ) had an aspect ratio closer to unity and showed a region of enlarged grains due to the thermal annealing after arc energy input. The microstructure

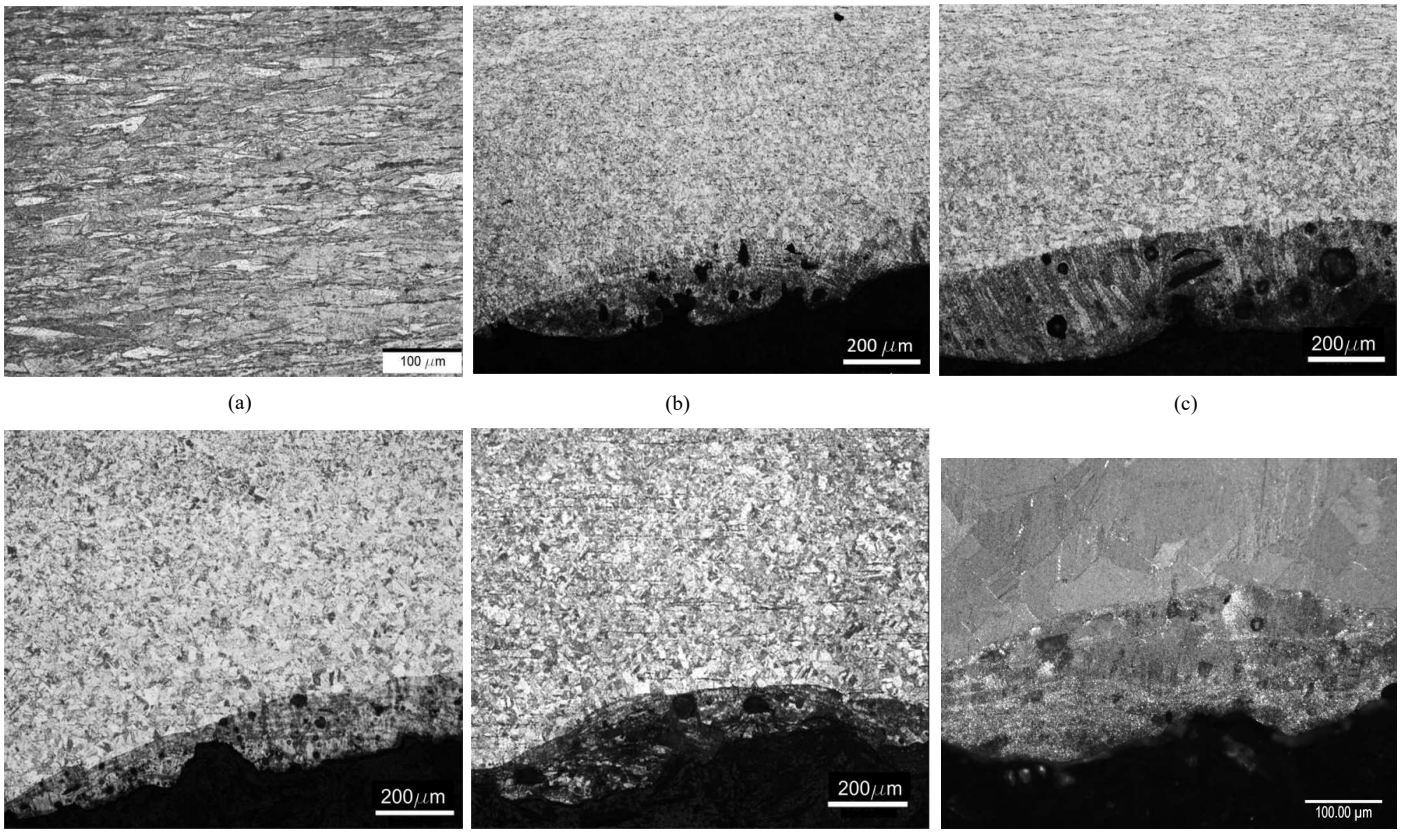

(a) (b) (c)

(d) (e) (f)

Figure 7 Microstructures of the contact wire samples, revealed by cross-sectioning the samples, polishing to a mirror finish and etching with a solution of 5 g FeCl3, 96 ml Industrial Methylated Spirit (IMS) and 2 ml HCl. (a) 100 A - Single Arc (T1) (b) 100 A - 10 repeated arcs (T2) (c) Arc-free (d) 200 A - Single Arc (T3) (e) 200 A - 10 repeated arcs (T4) (f) OFC 200 A- 10 repeated (T8)

of OFC tested with the 200A DC repeating arc is shown in Figure 7f. Although the arcing heat input visibly affected material to approximately 200µm below the contact wire surface, there was a significant reduction in large void formation in the damaged area. Since the OFC was not produced as wire the grain shape and its modification cannot be

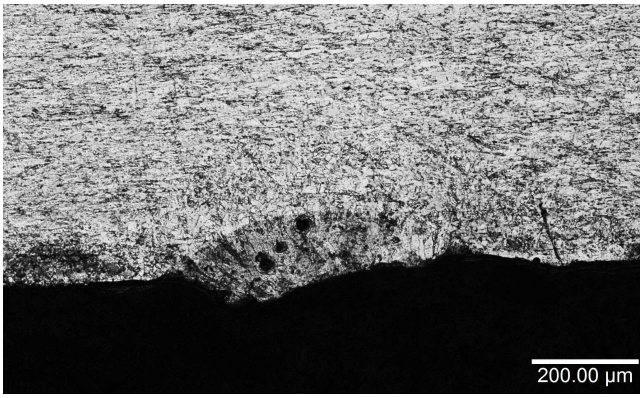

Figure 8 Microstructure of the contact wire section after single AC arcing (200A AC-(T6))

reliably used to deduce the penetration of heat into the wire

It was observed that the extinguishing times of the drawn AC arcs were shorter than those for the DC arcs, however, after testing with AC, the microstructure (*Figure 8*) showed similar features to those seen after testing with DC. Voids were formed in the tests with single and multiple arcs. In comparable tests, the HAZ was shallower for AC than for DC, corresponding to the reduced arc duration. Depending on the test condition the copper-silver contact wire was modified to a depth of 100-200 µm in AC and 200-300 µm in DC experiments and voids formed in this damaged zone.

To understand the geometry of the voids that were found in

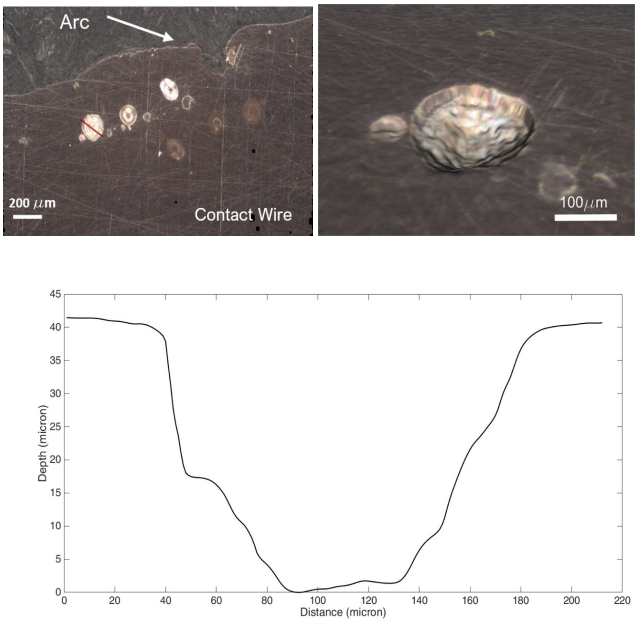

Figure 9 Surface and profile measurement of a void in test T4. (a) The location of the measured void relative to the arc exposure. (b) The topology of the void. (c) Profile of the void along the line indicated in red in (a)

microstructural inspections, a detailed 3D surface mapping was carried out for the sample of test T4. *Figure 9* shows microstructure, surface appearance and profile across a typical void from test T4. The 3D surface mapping showed that voids had a smooth interior surface with the diameter in the order of 40 µm in the damaged region.

C. *Post Arc Contact Wire Hardness*

Microhardness tests were performed for each of the samples with approximately 40 indents used to profile hardness from close to the surface to a depth of 2 mm. Three arc tests were conducted for each condition to verify the results. Three hardness traces for each of these samples were used to find the average hardness at each depth. For samples with voids or severely damaged surfaces, the measurements were started just below the severely damaged layer to avoid making unreliable measurements close to these internal defects.

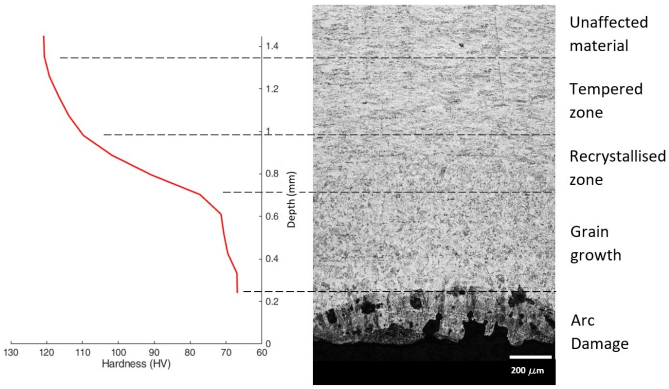

Figure 10 Hardness and regions of contact wire tested under the condition of T4

Figure 10 depicts the hardness of the contact wire tested under condition T4 and relates this to the microstructure at each depth. Wires tested under the other conditions examined had similar characteristics. In addition to regions of grain growth and recrystallised material (the visible HAZ) already discussed there was also a region of softened material, labelled ‘tempered zone’ with no visible distinction from the unaffected interior material. There was a clear trend of hardness decreasing from the interior parent material towards the heat-affected zone. The hardness of the grain growth region was significantly affected by the thermal exposure produced by the arcs. Although no grain growth was observed in the tempered zone arcing had still reduced the hardness of the material; a reduction in the order of 10% from the parent material.

The variation of hardness with depth from the surface for all the samples after arcing is shown in Figure *11*. To quantify the hardness results across tests the depth at which hardness was reduced to 80% of its core value is tabulated in Table 2. A similar softening pattern was seen for all of the samples with differences correlated with test conditions. Samples tested with DC current had greater penetration depth of hardness reduction than samples tested with AC current. Tests conducted with 200A DC current with a single arc exposure produced a hardness reduction of approximately 50 HV, taking it significantly below the ~120HV core hardness that it had had

prior to arc exposure. For DC tests of different currents greater depths of softening were produced by higher currents. For equal DC and AC RMS current, the AC tests produced damage over a smaller volume/depth of material than DC, reflecting the shorter duration of the arcs with AC.

Comparing the effect of single and multiple arcs no significant difference in the near-surface hardness reduction

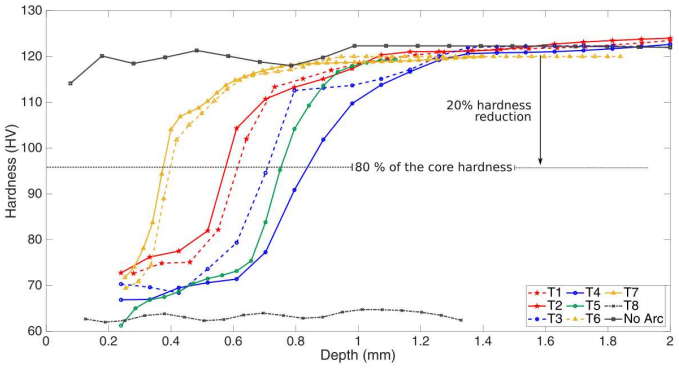

Figure 11 Hardness reduction for all test conditions

was found, with single and multiple arcs affecting samples in the same way. The depth of softening was marginally higher for repeated arc tests than for the corresponding single arc tests, but the overall finding was that the majority of the damage and softening can be generated by a single arc. Test condition T5 representing two pantographs on a single train producing rapid repetition of arcing generated similar hardness change to the other tests.

Data summarised in Table 2 shows that DC experiments resulted in larger grains compared to those following AC experiments. The largest grain size was measured as 0.0195 mm in the test of DC with 200A repeating arcs, this being close to that of arc-free samples subjected to the annealing process in test T9 (which had a grain size of 0.0202 mm). Because the microstructure of the contact wire contains different layers (arc damage, grain growth, recrystallisation, annealed and unaffected), these layers had different grain shapes and directions, therefore maximum grain size approach was used to express the modifications in the grains rather than average grain size.

Table 2 Hardness reduction and accumulated energy due to arcing

Test ID	Energy Input [kJ]	Hardness Reduction (at 0.24 mm depth) [%]	Depth for 80 % of core hardness [mm]	Max Grain Size (mm)
T1	1.35	39	0.61	0.0140
T2	1.17	39	0.58	0.0160
T3	1.56	41	0.75	0.0120
T4	1.59	44	0.82	0.0195
T5	1.30	49	0.75	0.0130
T6	0.030	43	0.39	0.0094
T7	0.045	41	0.37	0.0125
T9	-	-	-	0.0202

The energy input was calculated for a single arc using Joule heating law. According to the calculations of the thermal radiation loss, the heat per unit time lost by radiation in the contact wire was in the order of one in a thousandth of that going into the wire through joule heating. Thus, the heat lost by thermal radiation was neglected. One of the main reasons for this was because the area affected by intensive heating on the contact wire surface was minimal (approximately 20 mm^2). Also, the heat dissipating to a wider volume in the vicinity of this local region reduced absolute temperature, further reducing thermal radiation losses.

IV. Discussion

The equipment described in this paper has enabled the laboratory study of arc exposure for railway overhead contact wire materials with more control and greater ease than would be possible through on-site trials. The primary findings from the microstructural investigation of the tested samples were that (i) significant grain growth was observed in all samples after arc exposure, (ii) a recrystallised zone with completely revised grain shapes and a tempered zone (original grains but much softer) formed between the region of surface damage and unaffected base material and (iii) voids formed within 200-300 μm of the surface in both DC and AC experiments.

A consequence of arc damage to contact wires is the potential for accelerated wear in areas that have undergone softening, following Archard's relationship showing inverse proportionality of wear and hardness [31]. While wear can reduce the life of the wire it is a surface phenomenon so can be easily monitored by visual inspection. A local increase in wear rate by up to 50 % can be estimated by considering the inverse proportionality of wear and hardness in Archard's law. However, the regions of arc-softened material are small relative to the cross-section of the wire and the pantograph collector strip contact area, so surrounding unaffected material will mitigate the development of locally severe wear spots, thereby limiting the effect on overall service life of contact wire.

A more serious consequence is the initiation of fatigue damage within the wire. This is internal to the wire, so is much more difficult to observe or monitor. Line tension combined with uplift and bending of the contact wire as pantographs pass produces a stress cycle capable of driving fatigue crack propagation; this could eventually lead to sudden contact wire failure. Fatigue crack initiation from the voids observed close to the surface of arc affected specimens of contact wire was therefore of particular interest, and its investigation is reported elsewhere [32] showing that fatigue life in the arc damaged wires can be reduced by 50 % relative to undamaged wires under otherwise identical conditions. Given that growth of a fatigue crack is difficult to stop once it begins in a line under tension the question also arises of whether its initiation through void formation can be prevented.

The background to the formation of voids during exposure of copper to elevated temperatures was discussed in Section 1 in which hydrogen embrittlement was identified as a potential mechanism. This depends on the oxygen content of the copper which for a standard Cu-Ag contact wire is in the range 0.02 to

0.04% [31]. Oxygen-free copper for electrical applications typically contains one-hundredth of this level [26], [32] and may offer a route to avoid void formation, thereby closing off a route to fatigue crack initiation and subsequent contact wire failure. The initial test reported here on a sample of oxygen-free copper (test T8) demonstrated a significant reduction in voiding under arc exposure, supporting the possibility that use of oxygen free copper may lead to extended contact wire fatigue life. In this case, the sample was not produced as a contact wire so further work is required to fully understand the potential for this material when combined with the manufacturing process for the contact wire. In addition, its mechanical wear behaviour and its performance under combined sliding and electrical contact will require further investigation prior to deployment. A positive aspect is that electrical conductivity is enhanced in oxygen-free copper relative to conventional electrical copper, so there can be long term benefit of reduced electrical loses in addition to the potential for longer fatigue life.

V. Conclusion

Equipment is described and demonstrated for investigation of arc damage in railway contact wires, enabling cost-effective investigation of its impact on mechanical and metallurgical properties of the contact wire. The examples studied indicate the potential for reduction of arc damage seen in copper-silver wires by using oxygen-free copper (OFC) material. Increasing the current from 100 A to 200 A softened greater depths of the specimens, and longer arcs in DC cases produce more damage than for AC under similar conditions, but the effect of the number of arcs was not significant. Void formation was observed in arc exposed areas that has the potential to initiate fatigue failure under line tension and pantograph loading when in service. Although arc damage is unlikely to be a decisive factor in choice of AC or DC electrification the study demonstrates the potential for materials evaluation at a small scale in selecting contact wire materials expected to be subject to arc damage once in service.

Acknowledgement

Special thanks to Furrer+Frey and Network Rail for their support and collaboration, and to Chris Bryan for instigating the investigation and helpful discussion of the work. This project was also supported by the Turkish Ministry of National Education scholarship programme.

VI. References

[1] R. Stainton, “AC electrification with DC clearances,” London, 2015.
[2] J. Poza and J. M. Canales, “Mayr’s Equation-Based Model for Pantograph Arc of High-Speed Railway Traction System,” IEEE Trans. Power Deliv., vol. 25, no. 2, pp. 586–588, 2010.
[3] Z. Yang, Y. Zhang, F. Zhao, and B. Shangguan, “Dynamic variation of arc discharge during current-carrying sliding and its effect on directional erosion,” Tribol. Int., vol. 94, pp. 71–76, 2016.
[4] S. Barmada, M. Tucci, M. Menci, and F. Romano, “Clustering techniques applied to a high-speed train pantograph-catenary subsystem for electric arc detection and classification,” Proc. Inst. Mech. Eng. Part F J. Rail Rapid Transit, vol. 230, no. 1, pp. 85–96, 2016.
[5] X. Yu and H. Su, “Design and Simulation for Optical Acquisition of Pantograph-catenary Arcing Detection System of Electrified Railway,” IOP Conf. Ser. Mater. Sci. Eng., vol. 439, no. 5, pp. 3–8, 2018.
[6] S. Kubo and K. Kato, “Effect of arc discharge on wear rate of Cu-impregnated carbon strip in unlubricated sliding against Cu trolley under electric current,” Wear, vol. 216, no. 2, pp. 172–178, 1998.
[7] F. J. Gonzalez, J. A. Chover, B. Suarez, and M. Vazquez, “Dynamic analysis using finite elements to calculate the critical wear section of the contact wire in suburban railway overhead conductor rails,” Proc. Inst. Mech. Eng. Part F J. Rail Rapid Transit, vol. 222, no. 2, pp. 145–157, 2008.
[8] D. Hai He, R. R. Manory, and N. Grady, “Wear of railway contact wires against current collector materials,” Wear, vol. 215, no. 1–2, pp. 146–155, 1998.
[9] G. Bucca and A. Collina, “Electromechanical interaction between carbon-based pantograph strip and copper contact wire: A heuristic wear model,” Tribol. Int., vol. 92, pp. 47–56, 2015.
[10] W. Wang et al., “Experimental study of electrical characteristics on pantograph arcing,” 2011 1st Int. Conf. Electr. Power Equip. - Switch. Technol. ICEPE2011 - Proc., pp. 602–607, 2011.
[11] D. H. He, “Test Method of Arcing Behaviour for Railway Current Collection System,” Proc. Wold Congr. Railw. Res., no. poster 300, 2001.
[12] Y. Wang, Z. Liu, X. Mu, K. Huang, H. Wang, and S. Gao, “An Extended Habedank’s Equation-Based EMTP Model of Pantograph Arcing Considering Pantograph-Catenary Interactions and Train Speeds,” IEEE Trans. Power Deliv., vol. 31, no. 3, pp. 1186–1194, 2016.
[13] W. Wei et al., “Study on Pantograph Arcing in a Laboratory Simulation System by High-Speed Photography,” IEEE Trans. Plasma Sci., vol. PP, no. 99, pp. 2438–2445, 2016.
[14] H. J. Yang, G. X. Chen, G. Q. Gao, G. N. Wu, and W. H. Zhang, “Experimental research on the friction and wear properties of a contact strip of a pantograph-catenary system at the sliding speed of 350km/h with electric current,” Wear, vol. 332–333, pp. 949–955, 2015.
[15] S. Kubo and K. Kato, “Effect of arc discharge on the wear rate and wear mode transition of a copper-impregnated metallized carbon contact strip sliding against a copper disk,” Tribol. Int., vol. 32, no. 7, pp. 367–378, 1999.
[16] S. G. Jia, P. Liu, F. Z. Ren, B. H. Tian, M. S. Zheng, and G. S. Zhou, “Sliding wear behavior of copper alloy contact wire against copper-based strip for high-speed electrified railways,” Wear, vol. 262, no. 7–8, pp. 772–777, 2007.
[17] A. von Meier, Electric Power Systems: A Conceptual Introduction. Wiley, 2006.
[18] T. Ding, G. X. Chen, J. Bu, and W. H. Zhang, “Effect of temperature and arc discharge on friction and wear behaviours of carbon strip/copper contact wire in pantograph-catenary systems,” Wear, vol. 271, no. 9–10, pp. 1629–1636, 2011.
[19] G. -y. Zhu, G. -q. Gao, G. -n. Wu, Z. Gu, J. Wu, and J. Hao, “Modeling pantograph-catenary arcing,” Proc. Inst. Mech. Eng. Part F J. Rail Rapid Transit, vol. 230, no. 7, pp. 1687–1697, 2016.
[20] I. Zedin and S. Mnushkin, “Effect of oxygen on the susceptibility of copper to ‘hydrogen sickness,’” Met. Sci. Heat Treat., vol. 10, no. 3, pp. 184–185, 1968.
[21] P. K. Nagata, “Hydrogen Embrittlement of Tough Pitch Copper by Brazing,” 1975.
[22] M. R. L. Jr, “Hydrogen Embrittlement of Metals : A Primer for the Failure Analyst,” J. Fail. Anal. Prev., vol. 8, no. 3, pp. 289–307, 2008.
[23] J. Helavirta, “Oxygen-Free Copper for Industrial Applications,” 2019.
[24] Y. Feng, M. Zhang, and Y. Xu, “Effect of the electric current on the friction and wear properties of the CNT-Ag-G composites,” Carbon N. Y., vol. 43, no. 13, pp. 2685–2692, 2005.
[25] G. X. Chen et al., “Experimental study on the temperature of the contact strip in sliding electric contact,” Proc. Inst. Mech. Eng. Part J J. Eng. Tribol., vol. 231, no. 10, pp. 1268–1275, 2017.
[26] H. Nagasawa and K. Kato, “Wear mechanism of copper alloy wire sliding against iron-base strip under electric current,” Wear, vol. 216, no. 2, pp. 179–183, 1998.
[27] C. Tu, Z. H. Chen, and J. Xia, “Thermal wear and electrical sliding wear behaviors of the polyimide modified polymer-matrix pantograph contact strip,” Tribol. Int., vol. 42, no. 6, pp. 995–1003, 2009.
[28] BSI, “BS EN 50149: Railway applications — Fixed installations — Electric traction — Copper and copper alloy grooved contact wires,” 2012.
[29] ASTM, “B152- Standard Specification for Copper Sheet , Strip , Plate , and Rolled Bar 1,” pp. 1–8, 2011.
[30] ASTM, “ASTM E112-13: Standard test methods for determining average grain size,” ASTM Int., pp. 1–28, 2013.
[31] J. F. Archard, “Contact and rubbing of flat surfaces,” J. Appl. Phys., vol. 24, no. 8, pp. 981–988, 1953.
[32] O. Sunar, Arc Damage Identification and Its Effects on Fatigue Life of Contact Wires in Railway Overhead Lines (PhD Thesis). The University of Sheffield, 2020.